



Contents lists available at ScienceDirect

Cleaner Engineering and Technology

journal homepage: www.journals.elsevier.com/cleaner-engineering-and-technology

Oxidative torrefaction for cleaner utilization of biomass for soil amendment

Sonal K. Thengane^{a,b,c,*}, Kevin S. Kung^{a,f}, Ankita Gupta^e, Mohamed Ateia^d, Daniel L. Sanchez^b, Sanjay M. Mahajani^e, C. Jim Lim^f, Shahabaddine Sokhansanj^f, Ahmed F. Ghoniem^a^a Department of Mechanical Engineering, Massachusetts Institute of Technology, Cambridge, MA, USA^b Department of Environmental Science, Policy, & Management, UC Berkeley, Berkeley, CA, USA^c Hydro and Renewable Energy Department, Indian Institute of Technology Roorkee, Roorkee, India^d Department of Chemistry, Northwestern University, Evanston, IL, USA^e Department of Chemical Engineering, Indian Institute of Technology Bombay, Mumbai, India^f Department of Chemical and Biological Engineering, The University of British Columbia, Vancouver, BC, Canada

ARTICLE INFO

Keywords:

Biomass

Torrefaction

Oxidative

Soil amendment

Index of torrefaction

Biochar

ABSTRACT

Growing concerns of emissions from wildfires and burning of crop residues demand cleaner and efficient technologies to convert and utilize this residual biomass. The present study demonstrates a pilot scale moving bed biomass torrefaction reactor operating in oxidative medium to produce biochar for soil amendment. A series of experiments are conducted on pine shavings and rice husk, at conditions corresponding to different values of index of torrefaction (I_{torr}), ratio of higher heating value of torrefied biomass (i.e. biochar) to that of raw biomass. Air-biomass equivalence ratio dominantly governs the operating temperature and affects torrefaction more than the residence time. Product yields of scaled-up reactor differed from those of a smaller bench-top reactor, primarily because of differences in heat transfer within reactor and losses to the surrounding. A relatively linear relationship of I_{torr} is observed with biochar properties such as specific surface area, water retention capacity, bulk density, and electrical conductivity. When tested for soil amendment, the raw biomass and biochar treatments reduced soil pH by 0.2–0.3 in a season, with lowest pH values in case of pine shavings. Estimated nitrogen release and organic matter decreased with increasing I_{torr} , but most amendments had no significant effect on seed germination and the number of green shoots. Comparatively, heavy torrefied biomass treatments showed highest shoot heights and crop yield followed by light torrefied or raw biomass and control. Successful demonstration of a pilot scale reactor and encouraging effects on soil and plant growth suggest that commercial-scale oxidative torrefaction of various residual biomass is possible for soil amendment application.

1. Introduction

Biomass has gained significant interest among renewable energy sources, particularly in the sectors of energy, food, and water. Simultaneously, concerns have increased over the emissions and ecological losses because of wildfires and open burning of crop residues in different parts of world. For such residual biomass from agriculture and forestry, thermochemical processes such as gasification and different types of pyrolysis are widely applied. Torrefaction or mild pyrolysis is a thermochemical process that occurs in the range of 200–300 °C often at atmospheric pressure in limited or no oxygen presence. The process dries and partially devolatilizes biomass resulting in a solid product referred to as “torrefied biomass”, “biocoal” or “biochar” (Tumuluru et al., 2011). Torrefied biomass is known for its properties such as improved

hydrophobicity and grindability, high energy density and friability, and resistance to biodegradation, making it suitable for a range of applications (Bourgois and Guyonnet, 1988).

Biochar, a co-product of pyrolysis, incomplete combustion and gasification, has been proposed for applications ranging from soil amendment to water filtration (Barber et al., 2018), and as a solution to the issues of climate change and energy security (Thengane and Bandyopadhyay, 2020). Biomass heterogeneity, scattered availability, low density, high moisture, and associated logistics cost demands some pretreatment or processing at or near the source. In such situation, decentralized or mobile pyrolysis or torrefaction units could prove beneficial (Thengane et al., 2020a). In a typical pyrolysis process, low temperatures (<550 °C) favor production of bio-oil and bio-char while high temperatures (>550 °C) favor production of gas Yang et al. (2017).

* Corresponding author. Department of Mechanical Engineering, Massachusetts Institute of Technology, Cambridge, MA, USA. ,
E-mail addresses: sonalt@mit.edu, sonalt@hrc.iitr.ac.in (S.K. Thengane).

<https://doi.org/10.1016/j.clet.2020.100033>

Received 20 October 2020; Received in revised form 7 December 2020; Accepted 7 December 2020

2666-7908/© 2020 The Author(s). Published by Elsevier Ltd. This is an open access article under the CC BY license (<http://creativecommons.org/licenses/by/4.0/>).

pyrolyzed various woody biomass at 350–500 °C in a fixed bed tubular reactor under inert conditions and observed higher yields and HHV of biochar at lower temperatures Zambon et al. (2016). produced and physicochemically characterized the biochars made from olive and hazelnut pellets at 400 °C according to standards of European Biochar Certificate (EBC). Olive and hazelnut biochars had pH of 8.4 and 9.9, bulk density of 450 and 440 kg/m³, and electrical conductivity of 217 and 332 μS/cm. These properties ranked them in class of premium biochar, making them potential soil amenders Zhao et al. (2017). pyrolyzed apple tree branches at 300–600 °C in inert medium and studied structural and physicochemical properties of produced biochar. They observed higher BET surface area and pore volume at higher temperature primarily because of increase in surface area and volume of micropores. Also, thermal stability of biochars increased with increasing temperature because of increased fixed carbon and reduced volatiles, but yields and cation exchange capacity decreased Novak et al. (2009). described concept of designer biochar where the characteristics of biochar are matched to specific needs of a soil and/or soil management system. For example, certain high-pH biochars may be best for applying to acidic soils due to liming effect, and certain low-pH biochars may work better for alkaline soils.

Different factors such as process selection, reactor design, operation mode, biomass feedstock, and operating conditions determine the quality of biochar. Considering the available definitions of biochar based on carbon content and soil application contexts (Lee et al., 2019), torrefaction can produce biochars of different grades over a range of operating conditions. Though numerous studies investigated torrefaction in inert medium (Chen et al., 2015), some have explored the process in partially oxidative or oxygen-lean conditions because of potential energy and cost savings (Kung et al., 2019a). For oxidative torrefaction in a continuous moving bed reactor as discussed in (Kung et al., 2019b), air-biomass ratio is adjusted to maintain the reactor at desired temperature eliminating the need of any external energy supply. Most studies till now primarily focused on producing torrefied biomass as a fuel or a source of energy. Very few studies have focused on using it as biochar for soil amendment Ogura et al. (2016). found torrefied biomass as an effective soil amendment with enhanced moisture retention, structural stability and plant growth, and controlled soil microbes in Botswanaian arid soil Kwoczynski and Čmelík (2020). analyzed the nutrients content and thermal stability of various biochars produced by torrefaction of different biomass wastes, and found extracted rapeseed scrap to give the best biochar. A recent comparative study on biochar soil amendment found that torrefied biomass and a typical pyrolysis biochar had similar responses with respect to nitrogen except for higher uptake of phosphorus by torrefied biomass (Baldi et al., 2020). Lower nitrogen concentrations in feedstocks like agricultural residues can be retained in complex structures that do not easily volatilize in the temperature range of torrefaction (Gaskin et al., 2008). So far, a study on employing oxidative biomass torrefaction for soil amendment application is not evident in literature.

Our earlier studies described the concept of a laboratory-scale biomass torrefaction reactor for oxidative conditions (Kung et al., 2019a), mathematical model for the same (Kung and Ghoniem, 2019), modified index of torrefaction (Kung et al., 2020), and process parametric analysis for different biomasses (Kung et al., 2019b). These studies provided additional insights on reactor scale-up compared to many other laboratory-scale torrefaction reactors as it encapsulated more realistic elements of reactor performance and behavior that are crucial for scaling up the reactor. Later, we designed and fabricated a scaled-up version (i.e. 10–20 kg/h feed) of proposed reactor as a pre-commercial prototype for decentralized set-ups in agricultural farms and forestry (Thengane et al., 2020b). Torrefied biomass could be used for both energy and non-energy related applications preferably within the vicinity of production site. For instance, a medium sized mobile unit of 10 t/d feed capacity in a rural area with farmland of 100 acres can produce enough biochar for the entire area, and can supply surplus biochar to nearby areas.

Objective of present study is to test the designed moving bed

torrefaction reactor for different biomass in oxidative medium, understand effect of scaling, and investigate soil amendment by torrefied biomass. Pine shavings and rice husk are investigated at conditions corresponding to different values of index of torrefaction (I_{torr}). The produced torrefied biomasses are characterized for their composition and properties relevant to soil amendment. Finally, the influence of different raw and torrefied samples on soil quality and crop productivity is presented through a season long pot level experiment.

2. Material and methods

2.1. Reactor set-up

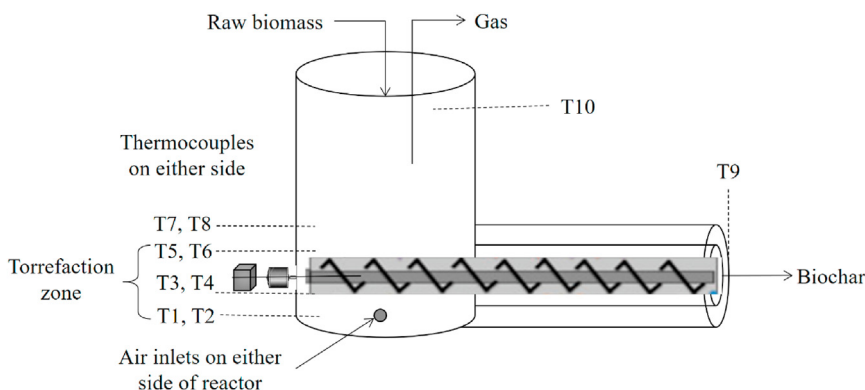
The reactor set-up involved a moving bed auger-based torrefaction unit where biomass fed from reactor top and flue gas generated primarily from combustion of volatiles move in a countercurrent mode, as shown in Fig. 1a (for actual set-up, please refer to appendix Figure A1). Main vertical cylindrical portion of reactor is about 1 m long having a diameter of 0.3 m. Horizontal char cooling segment is about 1 m long having two outlets with a diameter of 0.1 m each. Biomass is fed either using a feed auger or manually by a pre-weighed bucket at regular intervals maintaining a minimum level (e.g. 70–80% of reactor is always filled with biomass). Torrefied product is carried out of the reactor by the augers regulated through motor drive and the programmable logic controller (PLC). The speed of motor and auger controls the residence time (RT) of solid in reaction zone (temperature > 200 °C). Operation starts with ignition of some biomass, say pine shavings, in presence of excess air for a couple of minutes. More biomass is fed to extinguish the fire and air flow rate is gradually adjusted to a desired air-biomass equivalence ratio (ER), the ratio of actual mass flow rate of air to stoichiometric mass flow rate of air required for combustion of specific biomass (Kung, 2017). Thermocouples connected on both sides of reactor near highest temperature zone record real time temperatures to a LabJack datalogger connected to computer. It takes around 30–40 min for reactor to attain a steady state indicated by steady temperature profiles as shown in Fig. 1b and c. Unlike isothermal conditions in conventional inert torrefaction, oxidative torrefaction exhibits a temperature gradient with highest temperatures near air inlet (Thengane et al., 2020a). It is desirable to use air-biomass ER as a process parameter over temperature for oxidative torrefaction.

Similarly, for an auger-based reactor, it is difficult to have a constant residence time throughout the process because of improper mixing or heat and mass transfer affecting the load on the motor. During experiments, auger moved at variable speeds at certain instances, and had to be manually adjusted to the desired speed. The residence time is determined as average of all the measured time values during steady state condition. Start-up and shutdown periods of reactor are not considered for the experimental measurements. The steady state operation of reactor is considered for collection of torrefied biomass and for measuring different parameters in each experiment. Table 1 shows ultimate and proximate analysis, and HHVs of raw pine shavings and rice husks.

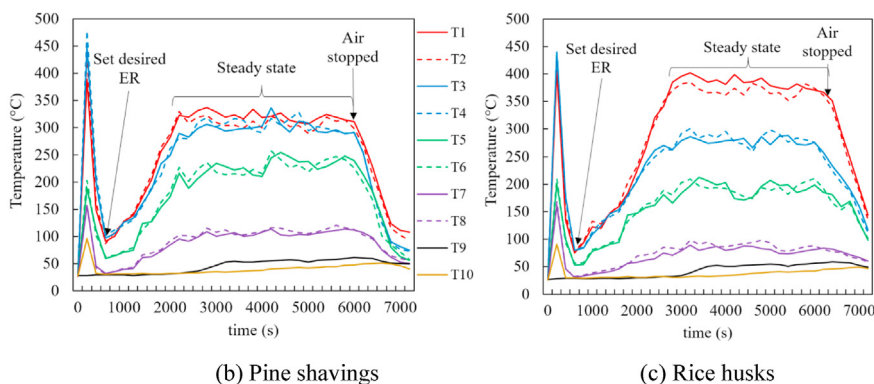
- (a) Thermocouple placements along height of the reactor (0.1 m apart along height on both sides of the reactor starting from bottom of the reactor)
- (b) Pine shavings (c) Rice husks

2.2. Measurements

The input solid mass flow rate is measured by weighing a bucket of raw biomass every 5 min using a digital balance (Dr. Meter ES-PS01) as an operator manually feeds that biomass in the reactor. Output solid mass flow rate is calculated from data collected by Arduino powered load cell (LCPW-20) holding the bucket for product char. The output from reactor is subjected to proximate analysis, ultimate (elemental) analysis, bomb calorimetry, and bulk density, BET surface area, and water retention capacity measurements. Experimental measurements of mass yields of



(a) Thermocouple placements along height of the reactor (0.1 m apart along height on both sides of the reactor starting from bottom of the reactor)



(b) Pine shavings

(c) Rice husks

Fig. 1. (a) Thermocouple placements in reactor; and temperature measurements along height of the reactor during torrefaction of: (b) pine shavings (RT: 15–20 min; ER = 0.11; $I_{\text{torr}} = 1.3$) and (c) rice husks (RT: 15–20 min; ER = 0.28; $I_{\text{torr}} = 1.3$) (The initial peak before 500 s occurs during reactor start-up when a small amount of biomass is combusted in excess air to heat up the reactor.).

Table 1

Ultimate analysis (dry basis), proximate analysis (as received basis), and HHV of biomass feedstock (C: Carbon; H: Hydrogen; O: Oxygen; N: Nitrogen; FC: Fixed carbon; VM: Volatile Matter; M: Moisture).

	Ultimate analysis				Proximate analysis				
	C	H	O	N	FC	VM	Ash	M	HHV (MJ/kg)
Pine shavings	46.6	6.5	46.80	0.01	6.43	88.5	0.27	4.8	21.9
Rice husks	37.2	5.1	57.45	0.25	14.3	66.6	14.1	5	15.8

solid product are within 1–2% error range.

As per ASTM D-3175 standard, proximate analysis measures the mass fractions of moisture, fixed carbon, volatile matter, and ash components in a given biomass sample. A thermogravimetry analyzer (TGA) (TA Instruments Q50) with EGA furnace and a digital mass balance is used to track mass loss of torrefied sample when heated to different temperatures. For volatile matter component, the procedure involves heating the biomass sample to 950 °C within 30 min and maintaining at that temperature for 7 min under inert condition of nitrogen. Remaining part of solid residue consists of fixed carbon and ash. In order to distinguish, the residue is subjected to an oxidative environment (air) at an elevated temperature of 600–750 °C so that the fixed carbon gets oxidized to gaseous carbon dioxide and water vapor. The residual matter left after this reaction is mainly ash (Kung et al., 2019b).

Ultimate or elemental analysis breaks down raw or torrefied biomass sample to its elemental components: mostly carbon, hydrogen, oxygen, and nitrogen (CHON), as per ASTM-D5373-16 protocol. The track record of number of different atoms entering and leaving the reactor helps to understand reaction chemistry, elemental composition, and outgoing volatiles. Ultimate analysis is carried out using a CHON analyzer

(Thermo Finnigan Flash EA 1112).

Higher heating values (HHVs) of raw and torrefied biomass samples are measured using a calorimeter (Parr Instrument Model 6200 isoperibol). The procedure involves grounding the prospective samples to small particles of sizes <0.5 mm, compressing to pellets using a manual pelleting press with a diameter of 0.64 cm and height of 0.25 cm (Parr Instrument 2810 series), and analysis in calorimeter. Index of torrefaction (I_{torr}) is the ratio of higher-heating value of torrefied biomass (HHV_{prod}) to higher-heating value of raw biomass (Kung et al., 2020). Different biomass, when subject to same torrefaction condition, may exhibit different degrees of energy densification, and different values of I_{torr} .

Bulk density of raw and torrefied biomasses is measured using ASTM-E873–82 protocol (Phanphanich and Mani, 2011) with slight modifications. The samples are first manually crushed and sorted to remove any lumps, and then poured in a standard 2000 mL cylindrical beaker from a height of 61 cm above the bottom edge of container. Beaker is gently shaken to uniformly spread the sample and flatten the top layer. Bulk density is calculated by the ratio of mass of sample to volume corresponding to height of sample in container. The bulk density of pine

shavings and rice husks is estimated to be 40 and 125 kg/m³.

Surface area of biomass species (grinded and passed through 200 μm sieve) is measured using BET (Brunauer–Emmett–Teller) (Model: Micrometics ASAP, 2020) sorptometer using nitrogen adsorption at -196 °C. All samples are initially degassed under vacuum for 10 h at 120 °C, so as to remove all adsorbed impurities. Due to samples' low surface area, measurements are performed with at least 3–4 g of each sample during the analysis. Samples are run in triplicates, and average of three readings is reported as the BET surface area of each sample.

To measure moisture or water retention capacity, 10 g of selected

torrefied biomass is submerged in 100 mL of water for a day under environmental conditions. The wet samples are carefully collected and weighed using a precision scale, before being dried in an oven at 100 °C for a day and cooled in a desiccator to be weighed later. Weight difference between wet and dried materials determined the mass of water retained in torrefied biomass. Water retention capacity is then calculated as a ratio of water weight to the torrefied biomass weight for each sample (Gondim et al., 2018).

For electrical conductivity measurement, grinded sample (torrefied biomass or soil) is air-dried and passed through a 200 μm sieve. 20 g of

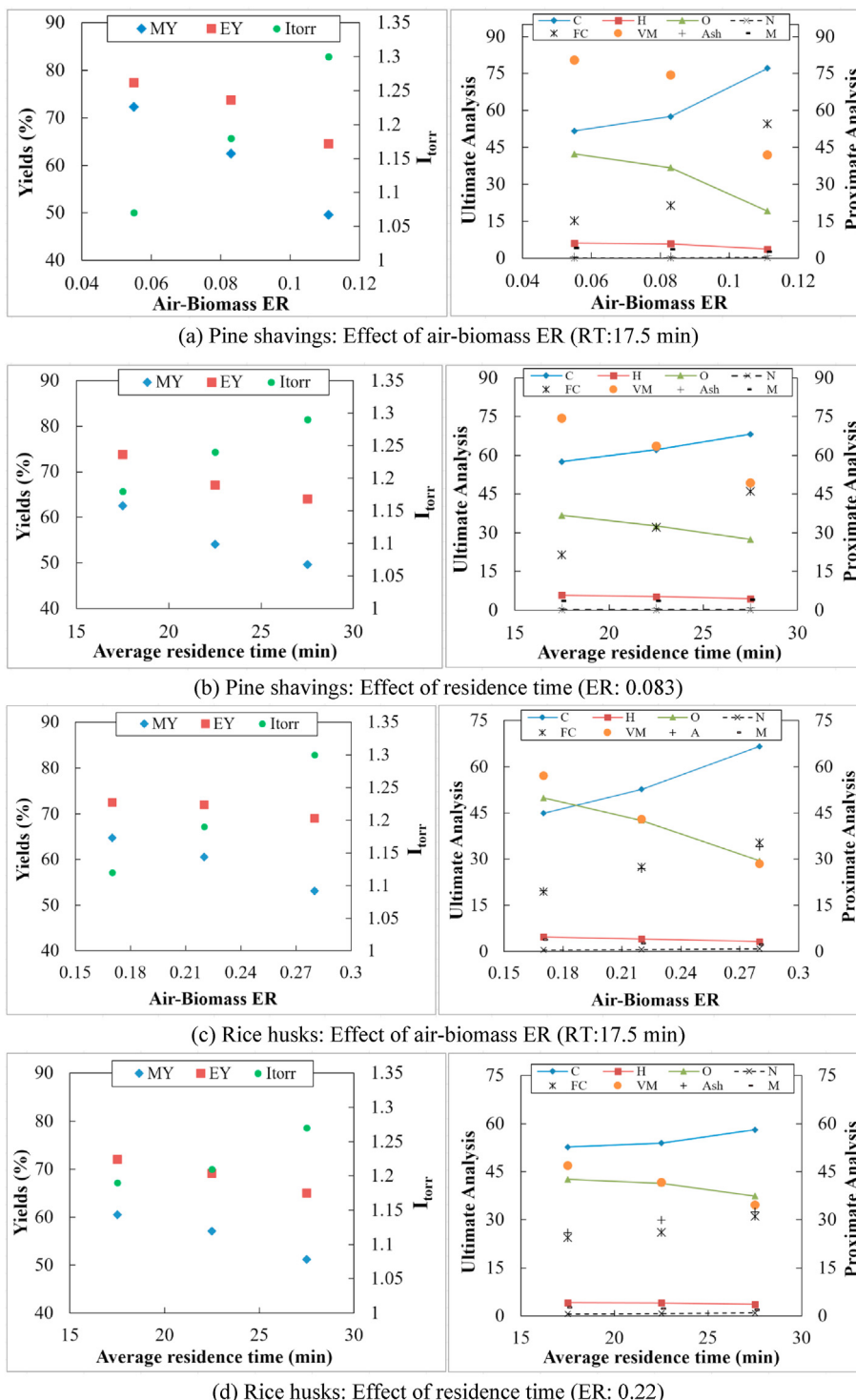


Fig. 2. Experimental results for torrefaction of pine shavings and rice husks at different conditions (Each point represent one experiment).

the sample is mixed with deionized water on 1:2 mass basis, stirred well, and left for 4 h. The solution is filtered through a Whatman No. 41 paper to collect the extract in a narrow beaker. Conductivity meter (Mettler Toledo Sevensgo SG3/51302530) is calibrated against 0.01 M and 0.1 M KCl solutions as standards, and then used to determine the electrical conductivity of the solution (Mylavarapu et al., 2020).

2.3. Soil amendment set-up

Series of pot experiments are performed at the MIT Bates laboratory in an enclosed space with open roof (please see appendix Figure A2) for investigating soil amendment. Each pot is filled with properly mixed 4 kg of soil batch (60% normal soil + 20% sand + 20% top soil). Normal soil is collected from a non-operational field in Massachusetts, USA, and sand and top soil are procured from the garden section of Home Depot. The objective is to check the impact of differently torrefied biomass on soil amendment. To test raw and two types of torrefied biomasses (light and heavy) for pine shavings and rice husks, 6 treatments are needed. The mixture without addition of raw or torrefied biomass served as a control. Each treatment, including control soil, is made in three replications resulting in total 21 pots arranged in a randomized block design. 40 g of raw or torrefied biomass (i.e. 1% application rate) is added to each of the 18 pots for 6 treatments. The torrefied biomass samples are grinded and the particle size in the range of 0.05–0.1 cm is selected. 25 wheat seeds procured from Johnny seeds, Maine are sown (5 seeds in 5 rows at fixed distances and 2.5 cm depth) in each of the 21 pots. Average 250 mL water is provided to all the pots on a daily basis. Positions of the pots are alternated every 2–3 days to minimize the effect of shading and positional bias. Experiments lasted for approximately 4 months, and soil samples are collected for analysis at the start, mid, and end of the experiment. Wheat plants are harvested after 4 months and mass of the grains is measured for each treatment. Soil analysis is carried out by A & L Western Agricultural Laboratories, California. Soil pH is measured on a weekly basis using Luster Leaf 1835 Rapitest digital soil analyzer. Few parameters of plant growth such as germination time, plant height, and number of shoot leaves, are also monitored at appropriate intervals of time.

3. Results and discussion

3.1. Torrefaction reactor

Fig. 2 show the experimental results for pine shavings and rice husks, mainly the effect of air-biomass ER and residence time on solid mass and energy yields, I_{torr} , and ultimate and proximate analyses of the torrefied biomass. Each point on graph corresponds to a single experiment conducted in two replicates to ensure reliable estimates. Few experiments with deviations greater than 10% in the yields were repeated thrice. For pine shavings, air-biomass ER values of 0.055, 0.083, and 0.111 correspond to air flow rates of 40, 60, and 80 LPM (liters per min). For rice husks, air-biomass ER values of 0.17, 0.22, and 0.28 correspond to air flow rates of 60, 80, and 100 LPM. For both biomasses, three residence time ranges of 15–20 min, 20–25 min, and 25–30 min correspond to average residence times of 17.5 min, 22.5 min, and 27.5 min. As air-biomass ER or residence time (RT) increases, the HHV of solid product, and the I_{torr} increases linearly for both biomasses, and, as expected, the mass and energy yields of torrefied biomass decreases. The corresponding change in each of the measured parameters is significant for a variation in ER than for RT. Air-biomass ER governing the temperature inside reactor operating in oxidative medium, is a dominant factor than the residence time, as in agreement with literature (Chen et al., 2015). The rates of decomposition of lignocellulosic components of biomass, especially hemicellulose, in torrefaction zone are governed by temperature more than the residence time. This is obvious from a simple kinetics model showing Arrhenius dependency on temperature and algebraic dependency on residence time for a first order reaction as

$$\frac{dc_A}{dt} = -kC_A = -A \exp\left(-\frac{E_a}{RT}\right)C_A \quad (1)$$

where C_A is concentration of feed, k is rate constant, A is pre-exponential factor, E_a is activation energy, R is molar gas constant, and T is temperature Strandberg et al. (2015). reported the temperature effect to be 1.3 to 1.9 times higher than the residence time effect on torrefaction of spruce wood. For a fixed air-biomass ER, longer residence time may achieve a higher degree of torrefaction but some fixed carbon would start to get consumed if biomass stays in the reactor longer than the time required for relatively quicker devolatilization reactions.

Ultimate analysis results show decreasing H/C and O/C ratios with increasing air-biomass ER and residence time. In this case too, drop in these ratios is higher with respect to air biomass ER than with respect to RT. FTIR results confirm that the intensities of O–H, C–H, C=C, C=O, and other bonds in torrefied biomass decrease with increasing torrefaction temperature and the ER (please see appendix Figure A3). With increasing torrefaction severity, the dehydroxylation and deoxygenation increases, and the removed oxygen is migrated primarily to H₂O followed by CO₂ and CO (Chen et al., 2018). For pine shavings, the fixed carbon content increased from 15.1% to 21.4% with increase in air-biomass ER from 0.055 to 0.083, but drastically increased to 54.6% at the air-biomass ER of 0.111. Similar observation is made with respect to decreasing volatile matter with increase in air-biomass ER. For all the experiments, solid mass yield is always lower than the corresponding energy yield as a significant fraction of mass loss consists of moisture and volatiles having relatively lower energy content than the carbon retained in solid product. Difference between solid mass and energy yields increased with increasing index of torrefaction. Moving from light to medium torrefaction (say, $I_{\text{torr}} = 1.05$ – 1.2), the changes in torrefaction performance (or the product properties) are gradual but from medium to severe torrefaction conditions (say, $I_{\text{torr}} > 1.2$), these changes are comparatively drastic. This holds true for residence time too except for the variations in the parameters are relatively lower.

- Pine shavings: Effect of air-biomass ER (RT:17.5 min)
- Pine shavings: Effect of residence time (ER: 0.083)
- Rice husks: Effect of air-biomass ER (RT:17.5 min)
- Rice husks: Effect of residence time (ER: 0.22)

Relative differences in case of two biomasses can be attributed to different chemical composition (please refer to Table 1) and properties. For example, HHVs of raw and torrefied samples of pine shavings are higher than those of corresponding samples of rice husks because of higher fixed carbon and volatile matter but significantly lower ash contents in pine shavings. To obtain a torrefied product of same severity (I_{torr} value), ER is almost 2.5 times for rice husk than for pine shavings. Variations in I_{torr} (or HHV), solid mass and energy yields, and ultimate and proximate analyses over a range of ER or RT are relatively lower for rice husks than for pine shavings because of lower lignocellulosic components (Wang et al., 2017) and approximately three times higher bulk density of rice husks than pine shavings. This difference in composition and properties of biomasses also result in the varying temperature gradients as shown in Fig. 1b and c. The closer values of thermocouples T1 to T4 in case of pine shavings is possibly because of higher quantity of volatiles released and oxidized during torrefaction due to less resistance by pine shavings. As highly dense rice husks offer high resistance to flow of volatiles and air in upward direction, the thermocouples in upper layer read substantially lower values than the lower ones.

The product of interest is solid (torrefied biomass), and the experimental set-up lacked arrangement for measuring gaseous and liquid yields. The heating values of gas leaving the reactor i.e. torgas are determined for few experiments based on the preliminary gas composition measurements using a portable rack type Infrared Syngas Analyzer Gasboard-3100. For highly torrefied ($I_{\text{torr}} = 1.3$) pine shavings and rice husks cases, average torgas lower heating values are found to be 2 and

1.5 MJ/kg (please see appendix Table A1). These values are substantially lower than for conventional inert torrefaction process (Chen et al., 2018), indicating that relatively more volatiles got oxidized within the reactor. Regarding liquid yield, if any tar is formed at the conditions of severe torrefaction, then heavier portions are most likely to either get deposited on the biomass particles and reactor walls or get oxidized. A study on rice husk torrefaction in inert medium observed about 65% of the liquid yield to be water with rest comprising of mainly acetic acid and tars (Chen et al., 2018). For oxidative torrefaction, percentage of water in liquid yield should be higher because of additional oxidation of volatiles and some fixed carbon in certain cases.

To study scale-up effect, yields from present reactor are compared to that of smaller reactor, at corresponding I_{torr} values for same feedstock, as shown in Fig. 3. Different scales of reactor may potentially encounter differences in heating rates and gas-solid interactions (Pawlak-Kruczek et al., 2017). For a scaled-up version of the bench-top reactor (0.1 m diameter and 0.4 m height) operating at same torrefaction severity, the mathematical model of Kung and Ghoniem (2019) predicted the mass yield to increase by 10–20%, attributing to reduction in relative heat losses as the incoming air flux is reduced by a factor of around 50% compared to smaller reactor. For pine shavings, solid mass and energy yields appear to be 5–10% higher for the bigger reactor, except for at very low I_{torr} values. For rice husks, the solid mass and energy yields appear to be 5–10% lower for the bigger reactor, except for one value of energy yield at severe torrefaction. This is because of the limitations of the model such as neglecting the thermal gradient in radial direction, which may be significant than anticipated as the reactor scales up. The transition of results from a smaller reactor to a scaled-up reactor is by no means straightforward, and should depend on several factors such as feedstock properties, operating conditions, fluid dynamics, and reactor design. This emphasizes the need for a detailed 2-D or 3-D model of a continuous torrefaction reactor operating in oxidative medium.

Since other objective of study is to test torrefied biomass as biochar for soil amendment application, it is important to investigate relevant properties. The particle size, shape, and internal structure of biochar play important roles in maintaining soil moisture because they alter net pore characteristics of the soil (Liu et al., 2017). Fig. 4a show BET surface area of raw and torrefied samples of pine shavings and rice husks plotted against I_{torr} . A relatively linear relationship is observed between surface area of torrefied biomass and I_{torr} with a satisfactory R^2 value (may improve with more data points). During torrefaction, more volatiles are released with increasing temperature or residence time, resulting in creation of more porous structure in biomass (Bouchelta et al., 2012). A slight decrease in case of pine shavings above I_{torr} of 1.3 at higher temperatures may be related to softening of lignin and cellulose present in higher proportions than in rice husks, and the onset of tar formation

deforming originally formed pores (Zheng et al., 2017).

Fig. 4b shows that water retention capacity (WRC) of torrefied pine shavings and rice husks decreases linearly with the increase in severity of torrefaction. WRCs of raw pine shavings and rice husks are 1.59 g/g and 1.03 g/g, decreases up to 1.1 g/g and 0.52 g/g for $I_{\text{torr}} = 1.3$. Rice husks have higher surface area but lower WRC than pine shavings. Though the increase in value of I_{torr} results in increased surface area, there exists no proven universal relationship between surface area and WRC of the wood chars (Zhang and You, 2013). One of the studies reported a drop in BET surface area of torrefied pine particle at 300 °C compared to that at 270 °C but rise in average pore size from 3 nm at 300 °C to 8.7 nm at 270 °C (Zheng et al., 2017). Water retention being an absorptive process is likely to depend also on porosity and particle size of material, but in this study, we used similar particle sizes for both biomasses. Earlier studies have correlated WRC with hydrophobicity, a property dependent on carboxylic groups on the solid surface, surface area and pore volume (Mao et al., 2019). For torrefied biomass, hydrophobicity known to increase with increasing temperature, is equivalent to decrease in the affinity of solid to absorb water. Rice husks have higher particle and bulk densities, and ash content than pine shavings, resulting in being more hydrophobic than pine shavings. A FTIR study on different torrefied biomass observed WRC to decrease with increasing hydrophobicity, but reported a critical temperature beyond which properties such as hydrophobicity change abruptly for torrefied biomass (Ibrahim et al., 2013). In conventional pyrolysis, hydrophobicity of biomass in process is found to increase with increase in temperature from 100 to 300 °C but decrease after 300 °C (Xiao et al., 2018). For I_{torr} values greater than 1.3, it is possible that torrefied pine shaving and rice husks show improvement in WRC. Operating at such severe conditions would result in much lower yields of torrefied biomass, and may not be preferred for a small increment in WRC. Next, we investigate bulk density and electrical conductivity of raw and torrefied samples.

Fig. 5a show the effect of torrefaction conditions on bulk densities of solid product for two biomasses. Raw pine shavings being highly compressible experiences higher rise in bulk density on torrefaction. Rice husk being much less compressible and denser, experiences a smaller rise in bulk density on torrefaction. Bulk density of torrefied pine shavings and rice husks increase gradually with increasing I_{torr} till $I_{\text{torr}} = 1.2$ but then it does not show significant variation. For both pine shavings and rice husks, torrefied product has a higher bulk density than raw biomass. Previous studies have observed similar effect for other biomass such as rice husk, bagasse, wheat straw (Saeed et al., 2015), and switchgrass (Sarkar, 2011). Another study found that the bulk density of torrefied pine chips decreased until the torrefaction temperature of 250 °C but then increased up to torrefaction temperature of 300 °C (Phanphanich and Mani, 2011). Increase in bulk density can be explained by relatively

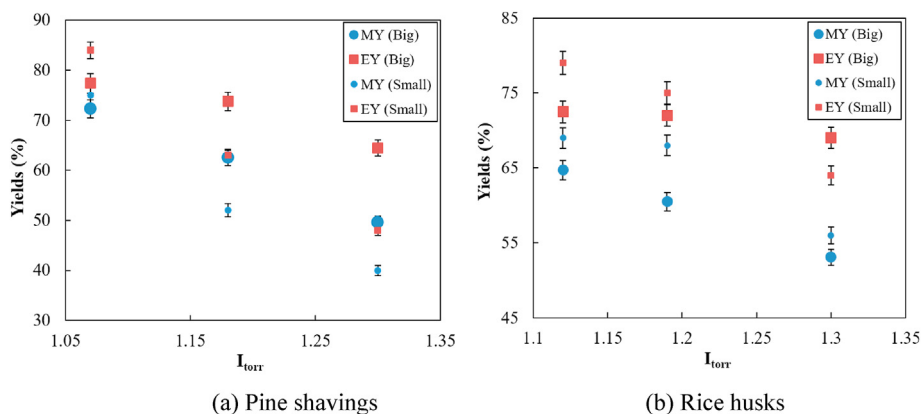


Fig. 2. Mass yield (MY) and energy yield (EY) at different torrefaction severities for reactors of different scales (Big: 10–20 kg/h lab-scale/pilot reactor (present study); Small: 1–2 kg/h bench-top reactor (Kung et al., 2019b)).

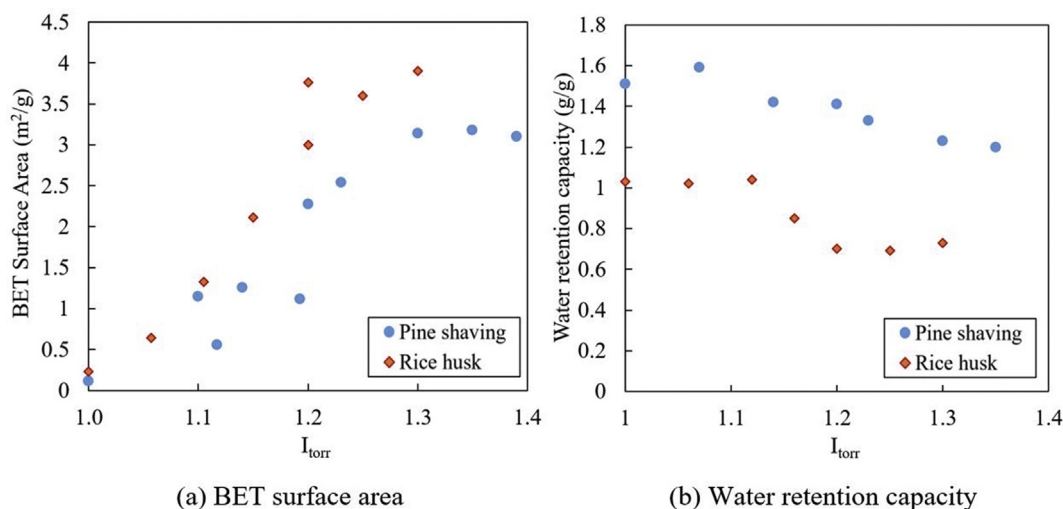


Fig. 4. BET surface area and water retention capacity of pine shavings and rice husk samples.

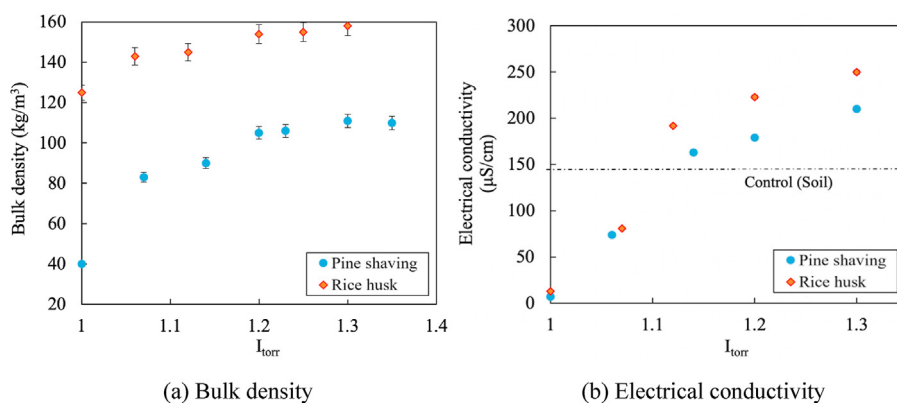


Fig. 5. Bulk densities of raw and torrefied pine shavings and rice husk samples, and electrical conductivities of selected samples.

higher volumetric reduction on release of moisture and volatiles than mass reduction. Another reason is decrease in particle size of torrefied product because of the impacts of attrition and auger blades, expected to increase the bulk density due to reduction in both inter- and intra-particle voids (Phanphanich and Mani, 2011).

Fig. 5b shows the effect of torrefaction conditions on the electrical conductivity (EC) of raw and torrefied biomasses. With increasing I_{torr} , EC of pine shavings and rice husks increased from 74 to 81 $\mu\text{S}/\text{cm}$ at $I_{\text{tor}} = 1.06$ to 210 and 250 $\mu\text{S}/\text{cm}$ at $I_{\text{tor}} = 1.3$. These values are substantially lower than for biochars (EC: 400–3000 $\mu\text{S}/\text{cm}$) produced during pyrolysis at temperatures higher than 400 °C (Ghorbani et al., 2019). The rise in EC of torrefied biomass is primarily because of increased carbon and mineral contents with increasing torrefaction temperature (Liu et al., 2018). This justifies relatively higher EC values of rice husks with higher ash content over pine shavings at similar operating conditions. Now that, surface area, water retention capacity, bulk density, and electrical conductivity of different raw and torrefied biomass samples are studied, we discuss the application of torrefied biomass produced from discussed reactor set-up as a biochar for soil amendment.

3.2. Soil amendment

To date, research and development on torrefied biomass has been predominantly for use in energy sector as a feedstock for gasification (Tumuluru et al., 2011), pyrolysis (Wannapeera and Worasuwannarak, 2015), and combustion (Niu et al., 2019). Torrefied biomass on grinding may resemble biochar of different grades depending on biomass

composition and treatment conditions. For soil amendment applications, high surface area and porosity of biochar increases its moisture and nutrient retention capacity, resulting in reduced water and fertilizer requirement (Kroeger et al., 2020). Lower N content and high compositional variability of biochar because of difference in operating conditions and feedstock make it a suitable conditioner for a variety of soils (Zhu et al., 2015). Soil analysis results for 7 treatments at start and end of the pot experiments are shown in the appendix Table A2. Addition of raw pine shavings and rice husks to soil increased estimated nitrogen release (ENR) and organic matter (OM) most, followed by light torrefied and heavy torrefied biomasses. Cation exchange capacity (CEC) of soil is found to reduce slightly in cases of pine shavings, and increase in case of rice husks. Though no conclusive observation could be made from the mineral components, decrease in mineral content except for potassium in all the samples by end of the season may be attributed to mineralization of soil organic matter (Weng et al., 2017) and the absorption by crop roots (Riedell and Schumacher, 2009). When light and heavy torrefied biomass samples are applied to soil at the rate of 1%, the treatments improved the EC of soil by 10–20% (please refer appendix Figure A4). A recent study attributed the improvements in root growth, uptake of N and P fertilizers, and crop production to biochar induced additions of soil carbon stocks and nutrients (Zhang et al., 2020). The treatments are also expected to increase water and nutrient retentions in soil because of improved surface area and porosity, and reduced bulk density. As discussed earlier, WRC of torrefied biomass is affected by its hydrophobicity but this may not have a significant effect on net soil WRC after incubation (Kameyama et al., 2019). Earlier studies have reported that the effect of

biochar on soil will not only depend on composition and operating conditions but also on the quality and properties of soil (Mao et al., 2019). Additionally, application rate of biochar (0.5–10%) will also determine overall impact on the soil quality and crop yield.

Fig. 6 shows the measurements of soil pH and mass of grains yielded after harvest for different treatments (please see appendix Table A3 for values). The slightly alkaline control soil dropped its pH from 7.35 to 7.30 at the end of 4 months. The significantly higher ash content of rice husk (12.4% ash on wet basis) than of pine shavings (0.27% ash on wet basis) is responsible for relatively higher pH of rice husk added soils at start of the season. All treatments with raw and torrefied biomasses reduced soil pH by 0.2–0.3 by end of the season. The extent of pH reduction is more in case of pine shavings because of higher fixed carbon and lower ash than rice husks. Mass yield of grains after harvest for all treatments increased with addition of raw and light torrefied biomasses in the range of 5–15%. Light torrefied biomass showed similar effect on mass yield of grains as that of untreated or raw biomass. A recent study reported biochar amendment to outperform raw biomass amendment in long term to enhance the biological carbon sequestration potential of both upland and paddy soils primarily because of increased microbial carbon use efficiency (Liu et al., 2020). In present study, heavy torrefied pine shavings showed 35.4% higher yield than control, and heavy torrefied rice husks showed 18% higher yield than control. This is interesting because torrefied rice husk showed better properties than torrefied pine shavings in most cases. This confirms that best biochar may not be a desired candidate for all types of soils and crops, and there is a need to identify biochar based on soil and crop requirements. In fact, some biochars under certain conditions could even have negative impact on the soil and crop growth (Adams et al., 2020). Few characteristics of torrefied pine shavings such as higher amount of fixed carbon and lower pH (6.6–6.8) could prefer alkaline soil as control and wheat crop. Optimum soil pH favorable for wheat growth has been reported as 6.4 and the general pH range is 6–7 (“Soil and Nutrient Management for Wheat,” 2015).

The timing and success rate of seed germination can be early indicators of effects of biochar quality on plant performance (Rogovska et al., 2012). In this study, wheat seeds germinated for all treatments between 20th and 21st day after seeding with one or two exceptions. Next week observed rising of green leafy shoots rising from all the pots. At the end of 28 days, number of green shoots were similar for most of the treatments except for heavy torrefied pine shavings with a couple of more shoots. When average height of leafy shoots was measured for each treatment on 29th day, heavily torrefied pine shavings and rice husks treatments showed largest heights (~9 cm) followed by raw biomass (~8.5 cm) and control (~6.5 cm). Though the number of samples tested are less for a single application rate, the observations highlight the potential of heavily torrefied biomass to amend soil properties and crop productivity more significantly than other samples. Overall amendment acted as an acidifying agent bringing down the pH of alkaline soil close to neutral regime. Different crops and plants prefer different levels of pH in the soil for their optimal growth (van Zwieten et al., 2010). Torrefied biomass or biochar with high pH ($\gg 7$) can be used as a liming agent to counteract soil acidification (Wang et al., 2014), and with low pH ($\ll 7$) can be used to reduce excess alkalinity of soil. High ash biomass such as rice husk may be ideal for making alkaline biochar unlike woody biomass with lower ash. However, for net alkaline effect, it is important that the amount of basic oxides in ash is higher than the amount of acidic oxides such as silica (Gupta et al., 2018).

Biochar can be used in a variety of soils as a standalone additive, a support for enzyme immobilization (Pandey et al., 2020), or can be mixed with alternatives such as compost, raw residues, or fertilizers (Guo et al., 2021). Application of biochar as soil amendment not only improves soil quality and productivity, but also offers an effective and a cleaner way of sequestering carbon in soil. Carbon in torrefied biomass or biochar is chemically and biologically more stable than in raw biomass (Manyà, 2012). For example, in case of heavy torrefied samples of rice

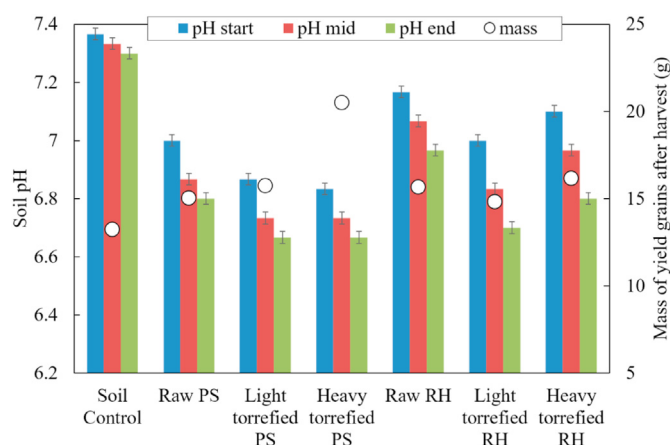


Fig. 6. Soil pH and mass of yield grains after harvest for different treatments (PS: pine shaving, RH: rice husk).

husk and pine shavings, emissions of 0.69 kg CO₂ and 1 kg CO₂ are saved per kg of raw RH and PS. Had these residues been burnt, it would have emitted 1.36 kg CO₂ and 1.71 kg CO₂ per kg of raw RH and PS. Utilization of torgas for energy purpose and improved growth of crops after biochar application would further save emissions through this cleaner technology. Though the detail analysis of carbon balance and GHG emissions is out of the scope of this study, these estimates prove the potential of torrefied biomass to sequester carbon in soil.

4. Conclusions

Oxidative torrefaction is proposed as a cleaner technology for converting residual biomass to biochar for soil amendment application. A pilot scale moving bed reactor is demonstrated for pine shavings and rice husks in oxidative medium at a wide range of operating conditions. Air-biomass ER dominates over residence time, affecting reactor temperature, HHV of solid product, and solid composition and yields. Scaled-up reactor did not replicate results from a smaller reactor in a straightforward way, as the performance depend on several other factors such as feedstock properties, operating conditions, fluid dynamics, and reactor design. The index of torrefaction (I_{torr}) showed a relatively linear relationship with specific surface area, water retention capacity, bulk density, and electrical conductivity of torrefied biomass (Table A4).

All soil amendment treatments except for control reduced soil pH by 0.2–0.3 by end of season, with higher extent of pH reduction in case of pine shavings than rice husks. The estimated nitrogen release (ENR) and organic matter (OM) increased most with addition of raw biomass followed by light torrefied and heavy torrefied biomasses. The onset of seed germination and number of green shoots did not change much, except for heavy torrefied pine shavings with relatively more shoots. Light or medium torrefied biomass showed similar effect on crop productivity as that of untreated biomass. It is important to choose a feedstock and operating conditions based on soil and crop requirements. Torrefied biomass resembling biochar, if used as soil amendment as a standalone substitute or in combination with compost and other fertilizers, not only improves soil quality and productivity, but also offers an effective way of sequestering carbon in soil. Other benefits include efficient management of residual biomass from agricultural and forestry sectors, avoiding them from being burnt leading to environmental emissions; and an additional source of income and employment for local community. Given that there is already a growing commercial interest in biochar, we believe that there is a significant scope in adapting and scaling this cleaner technology for decentralized biochar production from agricultural and forestry residues.

Acknowledgements

SKT would like to acknowledge MIT Abdul Latif Jameel Water and Food Systems Lab (J-WAFS) (Grant Number 6939696) and California

Department of Forestry and Fire Protection (Grant Number 70225) for funding and support. KSK would like to acknowledge MIT Tata Center Fellowship, Cyclotron Road Fellowship, and Natural Sciences and Engineering Research Council of Canada Postdoctoral Fellowship for support.

Appendix

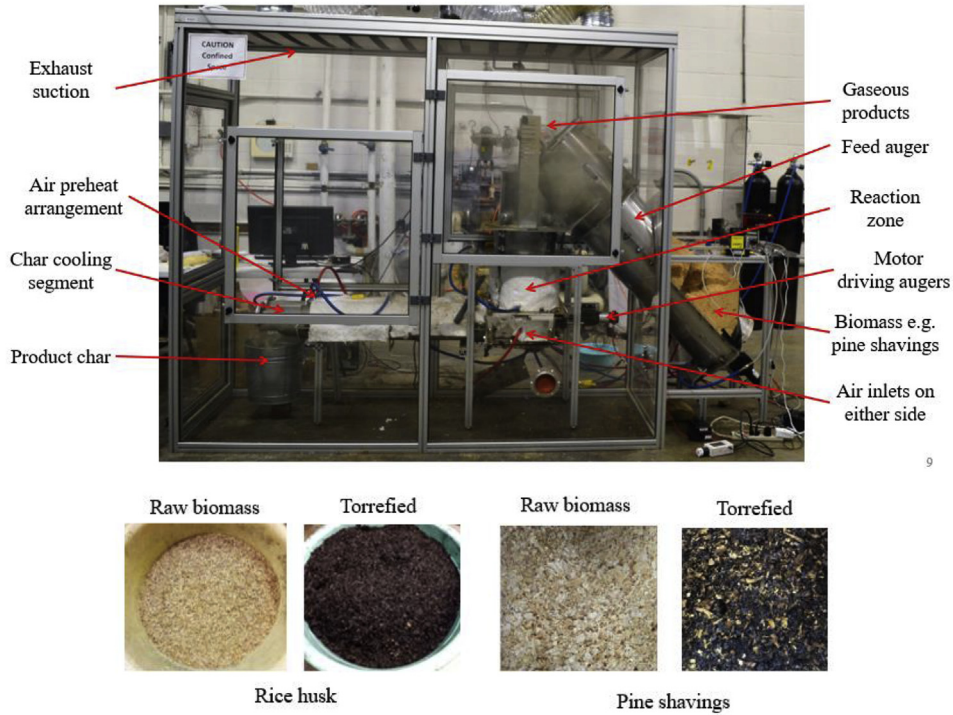


Fig. A1. Experimental set-up of pilot-scale moving bed reactor in laboratory, and the pictures of the biomass samples.



Fig. A2. Pot experiments for testing effect of raw and torrefied biomasses on soil.

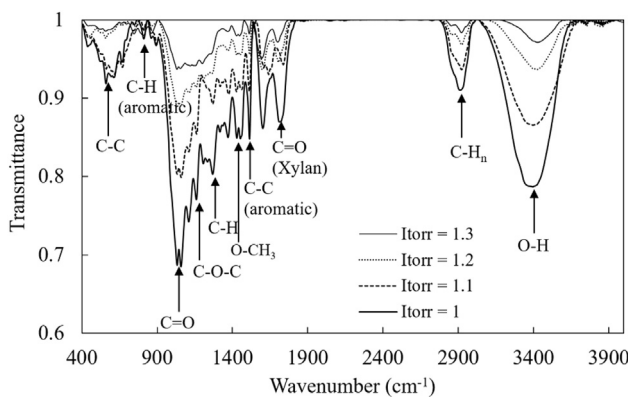


Fig. A3. FTIR of raw rice husk ($I_{torr} = 1$) and torrefied rice husks ($I_{torr} = 1.1-1.3$).

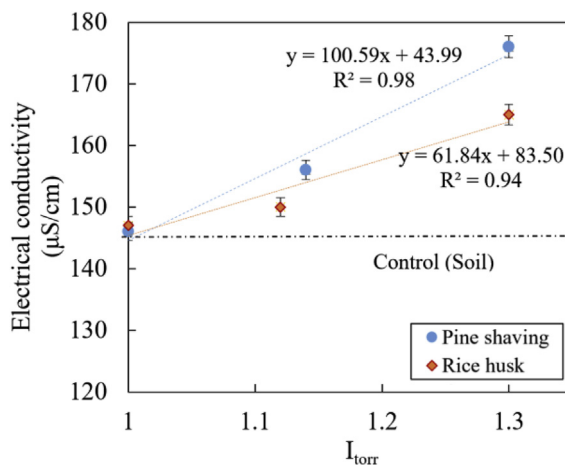


Fig. A4. Electrical conductivity results for control soil and treated soil with light and heavy torrefied biomass samples (Application rate: 1%).

Table A1

Torrefaction product distribution and torgas composition for a sample case of $I_{torr} = 1.3$ (RT = 17.5 min).

	Pine shavings (ER = 0.111)	Rice husks (ER = 0.28)
<i>Torrefaction product distribution (wt %)</i>		
Solid	49.6	53.1
Liquid + Gas	50.4	46.9
<i>Torgas composition (wt %)</i>		
CO ₂	43.2	41.5
CO	6	4.5
Other gases (CH ₄ , H ₂ , C ₂ H ₄)	2.5	1.8
H ₂ O	6.5	5.8
N ₂	41.8	46.4
Torgas calorific value/LHV (MJ/kg)	2.02	1.47

Table A2

Soil analysis results for start and end of the pot experiments

Sample	I_{torr}	ENR		OM		K		Mg		Ca		Na		CEC	
		Start	End	Start	End	Start	End								
Control	-	194	164	8.2	6.7	269	241	269	180	1273	1142	67.0	44.0	11.1	9.5
Raw PS	1	293	190	10.2	8	248	309	265	200	1255	1113	67.4	45.8	10.9	10.1
Light tor PS	1.1	282	166	9.4	6.8	259	261	231	179	1363	1090	62	41.5	10.7	9.8
Heavy tor PS	1.3	164	151	8.3	7.1	206	250	204	171	1291	1053	55.3	41.8	11.2	10.6
Raw RH	1	281	175	9.9	7.3	235	328	231	182	1314	1096	59.2	43.4	11.2	10.3
Light tor RH	1.1	207	184	8.9	7.7	263	273	242	181	1479	1159	63.4	41.6	11.4	9.6
Heavy tor RH	1.3	198	167	8.4	6.9	230	317	234	191	1499	1150	65.0	47.7	12.1	9.4

*(PS: pine shavings; RH: rice husks; tor: torrefied; ENR: estimated nitrogen release; OM: organic matter; K: potassium; Mg: magnesium; Ca: calcium; Na: sodium; CEC: Cation exchange capacity).

Table A3

Soil pH results and crop yield for all 21 samples at start, mid, and end of experiment

	Sample No.	Start	Mid	End	Mass of grains after harvest (g)
Soil control	1	7.4	7.3	7.3	14.0
	2	7.4	7.4	7.3	13.5
	3	7.3	7.3	7.3	12.2
Raw pine	4	6.9	6.8	6.7	15.0
	5	7.1	7	6.9	14.6
	6	7	6.8	6.8	15.5
Light torrefied pine	7	6.8	6.7	6.6	15.8
	8	6.9	6.8	6.7	17.1
	9	6.9	6.7	6.7	14.3
Heavy torrefied pine	10	6.8	6.7	6.6	21.4
	11	6.8	6.7	6.7	19.6
	12	6.9	6.8	6.7	20.5
Raw rice husk	13	7.1	7.1	7.0	15.0
	14	7.2	7.0	6.9	16.2
	15	7.2	7.1	7.0	15.8
Light torrefied rice husk	16	7.1	7	6.9	17.1
	17	7	6.8	6.6	13.2
	18	6.9	6.7	6.6	14.1
Heavy torrefied rice husk	19	7	6.8	6.6	15.5
	20	7.1	7.0	6.8	16.8
	21	7.2	7.1	7.0	16.2

Table A4

Data fit linear models for properties of pine shavings and rice husks for a range of I_{torr} .

Property (y)	Feedstock	Equation	R ²
BET surface area	Pine shavings	$y = 8.86x - 8.81$	0.87
	Rice husks	$y = 14.03x - 13.93$	0.93
Water retention capacity	Pine shavings	$y = -1.07x + 2.65$	0.88
	Rice husks	$y = -1.36x + 2.44$	0.77
Bulk density	Pine shavings	$y = 181.46x - 122.76$	0.79
	Rice husks	$y = 98.42x + 32.99$	0.87
Electrical conductivity	Pine shavings	$y = 678.26x - 646.62$	0.90
	Rice husks	$y = 805.62x - 765$	0.86

*y: property; x: I_{torr} .

References

- Adams, J.M.M., Turner, L.B., Toop, T.A., Kirby, M.E., Rolin, C., Judd, E., Inkster, R., McEvoy, L., Mirza, W.M., Theodorou, M.K., Gallagher, J., 2020. Evaluation of pyrolysis chars derived from marine macroalgae silage as soil amendments. *GCB Bioenergy* 12, 706–727. <https://doi.org/10.1111/gcbb.12722>.
- Baldi, H.D., Foster, T.L., Shen, X., Feagley, S.E., Smeins, F.E., Hays, D.B., Jessup, R.W., 2020. Characterization of novel torrefied biomass and biochar amendments. *Agric. Sci.* 11, 157–177. <https://doi.org/10.4236/as.2020.112010>.
- Barber, S.T., Yin, J., Draper, K., Trabold, T.A., 2018. Closing nutrient cycles with biochar from filtration to fertilizer. *J. Clean. Prod.* 197, 1597–1606. <https://doi.org/10.1016/j.jclepro.2018.06.136>.
- Bouchelta, C., Medjram, M.S., Zoubida, M., Chekkat, F.A., Ramdane, N., Bellat, J.P., 2012. Effects of pyrolysis conditions on the porous structure development of date pits activated carbon. *J. Anal. Appl. Pyrolysis* 94, 215–222. <https://doi.org/10.1016/j.jaap.2011.12.014>.
- Bourgeois, J., Guyonnet, R., 1988. Characterization and analysis of torrefied wood. *Wood Sci. Technol.* 22, 143–155. <https://doi.org/10.1007/BF00355850>.
- Chen, D., Gao, A., Ma, Z., Fei, D., Chang, Y., Shen, C., 2018. In-depth study of rice husk torrefaction: characterization of solid, liquid and gaseous products, oxygen migration and energy yield. *Bioresour. Technol.* 253, 148–153. <https://doi.org/10.1016/j.biortech.2018.01.009>.
- Chen, W.H., Peng, J., Bi, X.T., 2015. A state-of-the-art review of biomass torrefaction, densification and applications. *Renew. Sustain. Energy Rev.* 44, 847–866. <https://doi.org/10.1016/j.rser.2014.12.039>.
- Gaskin, J.W., Steiner, C., Harris, K., Das, K.C., Bibens, B., 2008. Effect of low-temperature pyrolysis conditions on biochar for agricultural use. *Trans. ASABE (Am. Soc. Agric. Biol. Eng.)* 51 (6), 2061–2069.
- Ghorbani, M., Asadi, H., Abrishamkesh, S., 2019. Effects of rice husk biochar on selected soil properties and nitrate leaching in loamy sand and clay soil. *Int. Soil Water Conserv. Res.* 7, 258–265. <https://doi.org/10.1016/j.iswcr.2019.05.005>.
- Gondim, R.S., Muniz, C.R., Lima, C.E.P., Santos, C.L.A., Dos, 2018. Explaining the water-holding capacity of biochar by scanning electron microscope images. *Revista Caatinga* 31, 972–979. <https://doi.org/10.1590/1983-21252018V31N420RC>.
- Guo, X., xia, Wu, biao, S., Wang, X., qing, Liu, tao, H., 2021. Impact of biochar addition on three-dimensional structural changes in aggregates associated with humus during swine manure composting. *J. Clean. Prod.* 280, 124380. <https://doi.org/10.1016/j.jclepro.2020.124380>.
- Gupta, A., Thengane, S.K.S., Mahajani, S., 2018. CO₂ gasification of char from lignocellulosic garden waste: experimental and kinetic study. *Bioresour. Technol.* 263, 180–191. <https://doi.org/10.1016/j.biortech.2018.04.097>.
- Ibrahim, R.H.H., Darvell, L.I., Jones, J.M., Williams, A., 2013. Physicochemical characterisation of torrefied biomass. *J. Anal. Appl. Pyrolysis* 103, 21–30. <https://doi.org/10.1016/j.jaap.2012.10.004>.
- Kameyama, K., Miyamoto, T., Iwata, Y., 2019. The preliminary study of water-retention related properties of biochar produced from various feedstock at different pyrolysis temperatures. *Materials* 12, 1–13.
- Kroeger, J.E., Pourhashem, G., Medlock, K.B., Masiello, C.A., 2020. Water cost savings from soil biochar amendment: a spatial analysis. *GCB Bioenergy* 25. <https://doi.org/10.1111/gcbb.12765>.
- Kung, K.S., 2017. Design and Validation of a Decentralized Biomass Torrefaction System. Massachusetts Institute of Technology, USA.
- Kung, K.S., Ghoniem, A.F., 2019. A decentralized biomass torrefaction reactor concept. Part II: mathematical model and scaling law. *Biomass Bioenergy* 125, 204–211. <https://doi.org/10.1007/s10530-005-5106-0>.
- Kung, K.S., Shanhogoe, S., Slocum, A.H., Ghoniem, A.F., 2019a. A decentralized biomass torrefaction reactor concept. Part I: multi-scale analysis and initial experimental validation. *Biomass Bioenergy* 125, 196–203. <https://doi.org/10.1007/s10530-005-5106-0>.
- Kung, K.S., Thengane, S.K., Ghoniem, A.F., 2020. Functional mapping of torrefied product characteristics with index of torrefaction. *Fuel Process. Technol.* 202, 106362. <https://doi.org/10.1016/j.fuproc.2020.106362>.
- Kung, K.S., Thengane, S.K., Shanhogoe, S., Ghoniem, A.F., 2019b. Parametric analysis of torrefaction reactor operating under oxygen-lean conditions. *Energy* 181, 603–614. <https://doi.org/10.1016/j.energy.2019.05.194>.
- Kwoczynski, Z., Čmelík, J., 2020. Characterization of biomass wastes and its possibility of agriculture utilization due to biochar production by torrefaction process. *J. Clean. Prod.* 280, 124302. <https://doi.org/10.1016/j.jclepro.2020.124302>.

- Lee, J., Sarmah, A.K., Kwon, E.E., 2019. Production and formation of biochar: fundamentals and applications. In: *Biochar from Biomass and Waste*. Elsevier, pp. 3–18.
- Liu, Z., Dugan, B., Masiello, C.A., Gonnermann, H.M., 2017. Biochar particle size, shape, and porosity act together to influence soil water properties. *PLoS One* 12, 1–19. <https://doi.org/10.1371/journal.pone.0179079>.
- Liu, Z., Niu, W., Chu, H., Zhou, T., Niu, Z., 2018. Effect of the carbonization temperature on the properties of biochar produced from the pyrolysis of crop residues. *BioResources* 13, 3429–3446. <https://doi.org/10.15376/biores.13.2.3429-3446>.
- Liu, Z., Wu, X., Liu, W., Bian, R., Ge, T., Zhang, W., Zheng, J., Drosos, M., Liu, X., Zhang, X., Cheng, K., Li, L., Pan, G., 2020. Greater microbial carbon use efficiency and carbon sequestration in soils: amendment of biochar versus crop straws. *GCB Bioenergy*. <https://doi.org/10.1111/gcbb.12763>.
- Manyà, J.J., 2012. Pyrolysis for biochar purposes: a review to establish current knowledge gaps and research needs. *Environ. Sci. Technol.* 46, 7939–7954. <https://doi.org/10.1021/es301029g>.
- Mao, J., Zhang, K., Chen, B., 2019. Linking hydrophobicity of biochar to the water repellency and water holding capacity of biochar-amended soil. *Environ. Pollut.* 253, 779–789. <https://doi.org/10.1016/j.envpol.2019.07.051>.
- Mylavarapu, R., Bergeron, J., Wilkinson, N., 2020. Soil pH and Electrical Conductivity: A County Extension Soil Laboratory Manual. University of Florida IFAS Extension, USA. <https://doi.org/10.32473/edis-ss118-2020>.
- Niu, Y., Lv, Y., Lei, Y., Liu, S., Liang, Y., Wang, D., Hui, S., 2019. Biomass torrefaction: properties, applications, challenges, and economy. *Renew. Sustain. Energy Rev.* 115, 109395. <https://doi.org/10.1016/j.rser.2019.109395>.
- Novak, J., Lima, I., Xing, B., Gaskin, J., Steiner, C., Das, K., Ahmedna, M., Rehrah, D., Watts, D., Busscher, W., 2009. Characterization of designer biochar produced at different temperatures and their effects on a loamy sand. *Ann. Environ. Sci.* 3, 195–206.
- Ogura, T., Date, Y., Masukujane, M., Coetzee, T., Akashi, K., Kikuchi, J., 2016. Improvement of physical, chemical, and biological properties of aridisol from Botswana by the incorporation of torrefied biomass. *Sci. Rep.* 6, 1–10. <https://doi.org/10.1038/srep28011>.
- Pandey, D., Davey, A., Arunachalam, K., 2020. Biochar: production, properties and emerging role as a support for enzyme immobilization. *J. Clean. Prod.* 255, 120267. <https://doi.org/10.1016/j.jclepro.2020.120267>.
- Pawlak-Kruczek, H., Krochmalny, K., Mościcki, K., Zgóra, J., Czerep, M., Ostrycharczyk, M., Niedźwiecki, L., 2017. Torrefaction of various types of biomass in laboratory scale, batch-wise isothermal rotary reactor and pilot scale, continuous multi-stage tape reactor. *Eng. Prot. Environ.* 20, 457–472. <https://doi.org/10.17512/ios.2017.4.3>.
- Phanphanich, M., Mani, S., 2011. Impact of torrefaction on the grindability and fuel characteristics of forest biomass. *Bioresour. Technol.* 102, 1246–1253. <https://doi.org/10.1016/j.biortech.2010.08.028>.
- Riedell, W.E., Schumacher, T.E., 2009. Transport of water and nutrients in plants. In: *Agricultural Sciences, vol. 1. Encyclopedia of Life Support Systems (EOLSS)*.
- Rogovska, N., Laird, D., Cruse, R.M., Trabue, S., Heaton, E., 2012. Germination tests for assessing biochar quality. *J. Environ. Qual.* 41, 1014–1022. <https://doi.org/10.2134/jeq2011.0103>.
- Saeed, M.A., Ahmad, S.W., Kazmi, M., Mohsin, M., Feroze, N., 2015. Impact of torrefaction technique on the moisture contents, bulk density and calorific value of briquetted biomass. *Pol. J. Chem. Technol.* 17, 23–28. <https://doi.org/10.1515/pjct-2015-0024>.
- Sarkar, M., 2011. Effects of Torrefaction and Densification on Devolatilization Kinetics and Gasification Performance of Switchgrass. Anna University, Chennai, India. <https://doi.org/10.1016/j.bbapap.2013.06.007>.
- Soil and Nutrient Management for Wheat, 2015. WestBred - Agronomic. Spotlight, vols. 1–2. Monsanto Company, USA.
- Strandberg, M., Olofsson, I., Pommer, L., Wiklund-Lindström, S., Åberg, K., Nordin, A., 2015. Effects of temperature and residence time on continuous torrefaction of spruce wood. *Fuel Process. Technol.* 134, 387–398. <https://doi.org/10.1016/j.fuproc.2015.02.021>.
- Thengane, S.K., Bandyopadhyay, S., 2020. Biochar mines: panacea to climate change and energy crisis? *Clean Technol. Environ. Policy* 22, 1–5. <https://doi.org/10.1007/s10098-019-01790-1>.
- Thengane, S.K., Burek, J., Kung, K.S., Ghoniem, A.F., Sanchez, D.L., 2020a. Life cycle assessment of rice husk torrefaction and prospects for decentralized facilities at rice mills. *J. Clean. Prod.* 275, 123177. <https://doi.org/10.1016/j.jclepro.2020.123177>.
- Thengane, S.K., Kung, K., York, R., Sokhansanj, S., Lim, C.J., Sanchez, D.L., 2020b. Technoeconomic and emissions evaluation of mobile in-woods biochar production. *Energy Convers. Manag.* 223, 113305. <https://doi.org/10.1016/j.enconman.2020.113305>.
- Tumuluru, J.S., Sokhansanj, S., Hess, R., Wright, C.T., Boardman, R.D., Hess, J.R., Kenney, K.L., Sokhansanj, S., Hess, J.R., Wright, C.T., Boardman, R.D., 2011. A review on biomass torrefaction process and product properties for energy applications. *Ind. Biotechnol.* 7, 1–19. <https://doi.org/10.1089/ind.2011.0014>.
- van Zwieten, L., Kimber, S., Morris, S., Chan, K., Downie, A., Rust, J., Joseph, S., Cowie, A., 2010. Effects of biochar from slow pyrolysis of papermill waste on agronomic performance and soil fertility. *Plant Soil* 327, 235–246. <https://doi.org/10.1007/s11104-009-0050-x>.
- Wang, L., Butterly, C.R., Wang, Y., Herath, H., Xi, Y.G., Xiao, X.J., 2014. Effect of crop residue biochar on soil acidity amelioration in strongly acidic tea garden soils. *Soil Use Manag.* 30, 119–128. <https://doi.org/10.1111/sum.12096>.
- Wang, S., Dai, G., Yang, H., Luo, Z., 2017. Lignocellulosic biomass pyrolysis mechanism: a state-of-the-art review. *Prog. Energy Combust. Sci.* 62, 33–86. <https://doi.org/10.1016/j.pecs.2017.05.004>.
- Wannapeera, J., Worasuwannarak, N., 2015. Examinations of chemical properties and pyrolysis behaviors of torrefied woody biomass prepared at the same torrefaction mass yields. *J. Anal. Appl. Pyrolysis* 115, 279–287. <https://doi.org/10.1016/j.jaap.2015.08.007>.
- Weng, Z., Han, J., Van Zwieten, L., Singh, B.P., Tavakkoli, E., Joseph, S., Macdonald, L.M., Rose, T.J., Rose, M.T., Kimber, S.W.L., Morris, S., Cozzolino, D., Araujo, J.R., Archanjo, B.S., Cowie, A., 2017. Biochar built soil carbon over a decade by stabilizing rhizodeposits. *Nat. Clim. Change* 7, 371–376. <https://doi.org/10.1038/nclimate3276>.
- Xiao, X., Chen, B., Chen, Z., Zhu, L., Schnoor, J.L., 2018. Insight into multiple and multilevel structures of biochars and their potential environmental applications: a critical review. *Environ. Sci. Technol.* 52, 5027–5047. <https://doi.org/10.1021/acs.est.7b06487>.
- Yang, X., Wang, H., Strong, P.J., Xu, S., Liu, S., Lu, K., Sheng, K., Guo, J., Che, L., He, L., Ok, Y.S., Yuan, G., Shen, Y., Chen, X., 2017. Thermal properties of biochars derived from waste biomass generated by agricultural and forestry sectors. *Energies* 10, 1–12. <https://doi.org/10.3390/en10040469>.
- Zamboni, I., Colosimo, F., Monarca, D., Cecchini, M., Gallucci, F., Proto, A.R., Lord, R., Colantoni, A., 2016. An innovative agro-forestry supply chain for residual biomass: physicochemical characterisation of biochar from olive and hazelnut pellets. *Energies* 9, 1–11. <https://doi.org/10.3390/en9070526>.
- Zhang, J., You, C., 2013. Water holding capacity and absorption properties of wood chars. *Energy Fuels* 27, 2643–2648. <https://doi.org/10.1021/ef4000769>.
- Zhang, Q., Song, Y., Wu, Z., Yan, X., Gunina, A., Kuzyakov, Y., Xiong, Z., 2020. Effects of six-year biochar amendment on soil aggregation, crop growth, and nitrogen and phosphorus use efficiencies in a rice-wheat rotation. *J. Clean. Prod.* 242, 118435. <https://doi.org/10.1016/j.jclepro.2019.118435>.
- Zhao, S.X., Ta, N., Wang, X.D., 2017. Effect of temperature on the structural and physicochemical properties of biochar with apple tree branches as feedstock material. *Energies* 10. <https://doi.org/10.3390/en10091293>.
- Zheng, Y., Tao, L., Yang, X., Huang, Y., Liu, C., Gu, J., Zheng, Z., 2017. Effect of the torrefaction temperature on the structural properties and pyrolysis behavior of biomass. *BioResources* 12, 3425–3447. <https://doi.org/10.15376/biores.12.2.3425-3447>.
- Zhu, Q., Peng, X., Huang, T., 2015. Contrasted effects of biochar on maize growth and N use efficiency depending on soil conditions. *Int. Agrophys.* 29, 257–266. <https://doi.org/10.1515/intag-2015-0023>.